Japanese Journal of Applied Physics
Vol. 46, No. 7B, 2007, pp. 4889–4896

Ultrasonic Imaging of Propagation of Contraction and Relaxation in the Heart Walls at High Temporal Resolution

Hiroki YOSHIARA, Hideyuki HASEGAWA, Hiroshi KANAI*, and Motonao TANAKA[1]

Graduate School of Engineering, Tohoku University, Sendai 980-8579, Japan
[1]*Tohoku Welfare Pension Hospital, Sendai 983-8512, Japan*

(Received November 24, 2006; revised March 6, 2007; accepted March 22, 2007; published online July 26, 2007)

Strain and strain rate imaging have been shown to be useful for the assessment of regional myocardial function. However, some of the mechanisms of transition in myocardial contraction/relaxation remain unclear. In this study, the RF echoes from the left ventricular (LV) wall were acquired in both the longitudinal-axis view and the apical view by scanning ultrasonic beams sparsely to improve the temporal resolution, and a frame rate of about 600 Hz was realized. The *phased tracking method* was applied to multiple points in the heart wall to estimate the strain rate. The spatial distribution of the strain rate measured about every 2 ms showed the continuous transition in the myocardium. In the apical view, the propagation speed of contraction from the apex to the base side in the interventricular septum was found to be about 0.8 m/s. These results indicate the potential of this method in the estimation of the physiological function of the myocardium.
[DOI: 10.1143/JJAP.46.4889]

KEYWORDS: myocardial contraction/relaxation, strain rate, phased tracking method, frame rate, *in vivo* experiments

1. Introduction

In recent years, there have been many studies on the measurement of myocardial strain or strain rate, and techniques for measuring them have been developed. However, some of the mechanisms of the transition in myocardial contraction/relaxation still remain unclear.

In conventional echocardiography, we can see mainly the shapes of organs and their slow motion with large amplitude. In this case, the frame rate is, at most, 50 Hz, which corresponds to the sampling period of 20 ms.

For noninvasive measurement of the heart wall, tissue Doppler imaging (TDI) has been developed.[1–6] The TDI technique enables the determination of the motion distribution in the myocardium in real time. In this method, the frame rate in TDI is limited to 200 Hz,[1] corresponding to the sampling period of 5 ms. However, some transitions rapidly occur during a short period of about 10 ms.[7,8] Therefore, the continuous observation of such short transition requires a frame rate of more than 200 Hz. In this study, ultrasonic beams were scanned sparsely so that the myocardial strain rate could be measured in a wide area at a high temporal resolution of about 1/600 s, particularly during the period from the R-wave in the electrocardiogram (ECG) to the second heart sound in the phonocardiogram (PCG).

To improve the spatial resolution, Kanai *et al.* proposed the *phased tracking method* which enables the detection of small vibrations in the heart wall.[9] This method was applied to multiple points preset in the left ventricular (LV) wall along an ultrasonic beam so that the spatial distribution of velocities at those points is simultaneously obtained.[10,11] Furthermore, this method was applied to other applications, such like the measurements of ultrasound backscatter[12] and heart wall vibrations induced by external actuation.[13] In this study, the *phased tracking method* was applied to the points assigned along the ultrasonic beam at smaller intervals than those in the previous studies[10,11] to obtain a more continuous distribution of the myocardial strain rate along an ultrasonic beam.

In addition, the LV wall was measured not only in the long-axis view[8] but also in the apical view. *In vivo* experimental results in each scanned plane showed spatial transition in myocardial contraction/relaxation. These results showed the possibility of applying this method in the elucidation of the mechanism of myocardial contraction/relaxation.

2. Principles

As illustrated in Fig. 1, both the interventricular septum (IVS) and posterior wall were measured. The RF data were acquired using a 3.75 MHz sector-type probe of ultrasonic diagnostic equipment (ALOKA SSD-6500). The sampling frequency of the RF signal was 15 MHz. At time $t = t_0$, which is at the center of the assigned time period for analysis, N layers with a thickness of $\Delta d = 821\,\mu$m were assigned in the IVS from the right ventricular (RV) side to

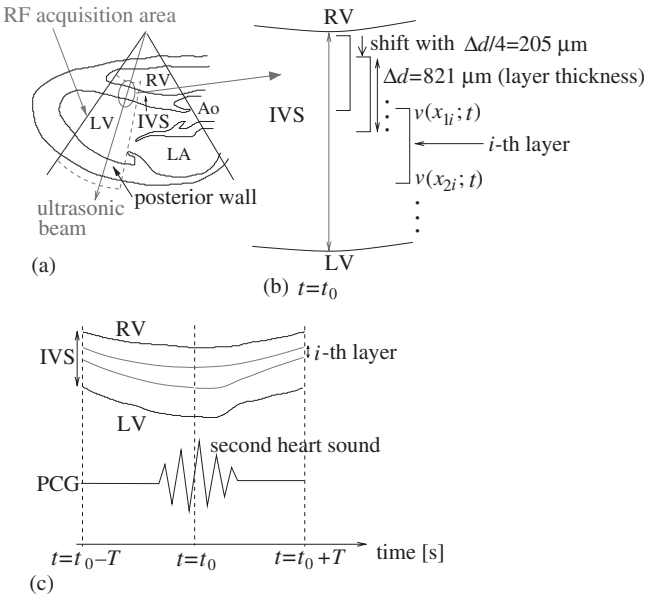

Fig. 1. (a) RF signal acquisition in the parasternal longitudinal-axis view of the LV. (b) Method of assigning layers along an ultrasonic beam at $t = t_0$. (c) Application of *phased tracking method* to the points preset in the heart wall at $t = t_0$.

*E-mail address: hkanai@ecei.tohoku.ac.jp

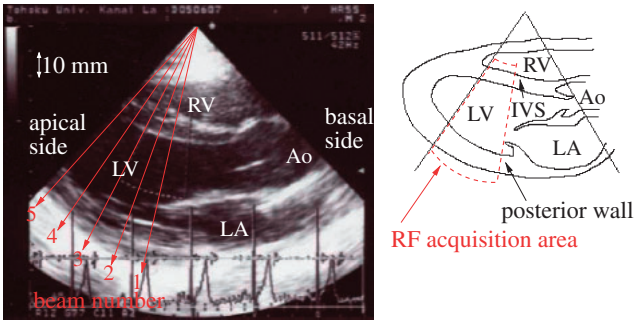

Fig. 2. Cross-sectional image of the left ventricle in the long-axis view obtained by conventional echocardiography for a healthy 22-year-old male. The red arrows show the direction of the five ultrasonic beams used for the estimation of strain rate in the IVS and posterior wall.

the LV side along an ultrasonic beam with intervals of $\Delta d/4 = 205\,\mu\text{m}$. The thickness Δd was determined from the duration of an ultrasonic pulse transmitted from the probe. Then, the *phased tracking method* was applied to both the top x_{1i} and the bottom x_{2i} of the i-th layer ($i = 0, 1, 2, \ldots, N-1$) to estimate velocities, $v(x_{1i}; t)$ and $v(x_{2i}; t)$, for the period, $t_0 - T \leq t \leq t_0 + T$. Period T was set as short as possible to avoid the influence of lateral motion of the heart wall,[14] which is perpendicular to the ultrasonic beams.

We introduced the strain rate to evaluate how the thickness of each layer changes with respect to time. Strain rate $S_i(t)$ of the i-th layer from the RV surface ($i = 0$) at time t is given by[10]

$$S_i(t) = \frac{v(x_{2i}; t) - v(x_{1i}; t)}{\Delta d} \quad [(\text{m/s})/\text{m}], \qquad (2.1)$$

The numerator shows the difference between velocities at the top and bottom points of the i-th layer, and the denominator shows the initial thickness of the layer for normalization. After the strain rates were estimated along each ultrasonic beam, they were superimposed on the B-mode image in every frame using a color code to obtain the two-dimensional (2-D) spatial distribution of the strain rate. Blue indicates a thickening layer caused by myocardial contraction, and red indicates a thinning layer caused by myocardial relaxation. The strain rate of the posterior wall was estimated as well as that of the IVS.

3. *In vivo* Experimental Results

3.1 *Transition from R-wave to second heart sound in long-axis view*

Figure 2 shows a typical cross-sectional image (the transthoracic parasternal longitudinal-axis view) of the heart obtained from a healthy 22-year-old male. The figure on the right-hand side of Fig. 2 shows the RF acquisition area. In the acquisition of RF signals, the ultrasonic beam scans only 5 different directions sparsely to maintain a high temporal resolution. The frame rate was set to 630 Hz.

Figure 3 shows the two-dimensional distribution of strain rate in the same subject as shown in Fig. 2 during the transient period from contraction to relaxation. The bottom graph shows the temporal change in the width of the LV chamber along each ultrasonic beam. In the isovolmic contraction phase [Fig. 3(b)], the basal side of the IVS decreases in thickness, which corresponds to the extension

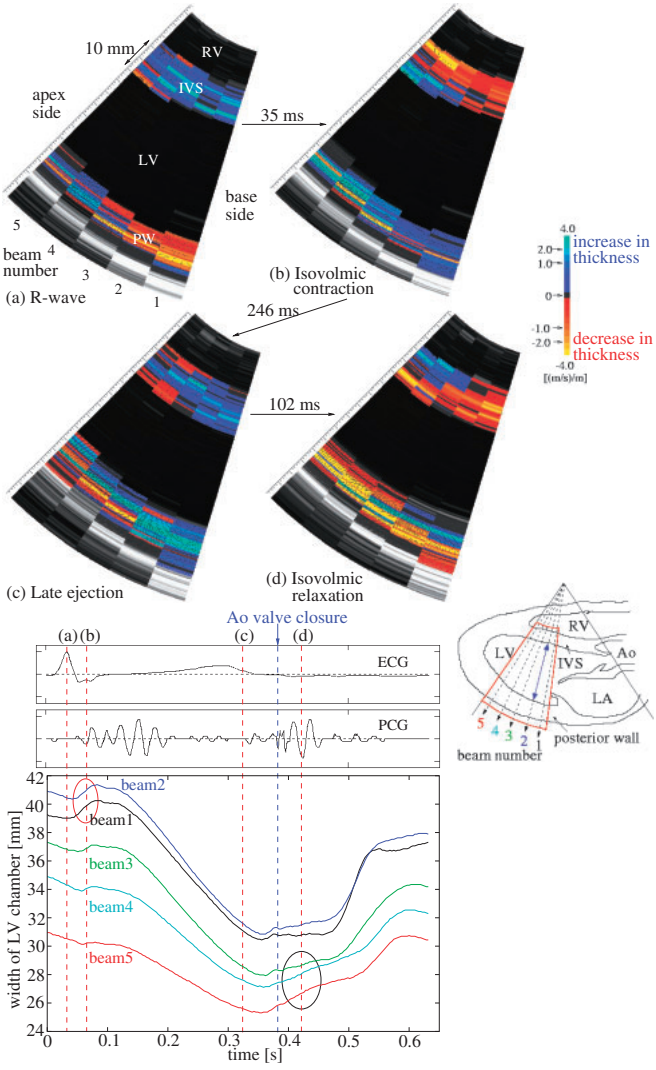

Fig. 3. Two-dimensional distribution of strain rate in the long-axis view from the R-wave to the second heart sound for the same subject as in Fig. 2. (a) Time of the R-wave. (b) Isovolmic contraction phase. (c) Late ejection phase. (d) Isovolmic relaxation phase. The bottom graph shows the temporal change in the width of the LV chamber along each beam.

of the LV chamber at the basal area, as indicated by the red oval in the graph. This is considered to result from an increase in the LV pressure upon contraction at the apical area for the succeeding ejection phase. Figures 3(b) and 3(c) show that the contraction extends gradually from the apical area to the basal area in the posterior wall. In addition, it is found that the apical area of the posterior wall begins to relax in the late ejection phase [Fig. 3(c)]. In the isovolmic relaxation phase [Fig. 3(d)] after aortic (Ao) valve closure,[15] the posterior wall at the apical area relaxes rapidly, which corresponds to the extension of the LV chamber at the apical area, as indicated by the black oval in the graph at the bottom of Fig. 3. This action is considered to cause the reduction of the LV pressure for the succeeding rapid filling phase. These preceding actions for the subsequent phases probably contribute to the efficient pump function of the left ventricle.

3.2 *Transition from contraction to relaxation around second heart sound in long-axis view*

Figure 4 shows the strain rate distribution in the myocar-

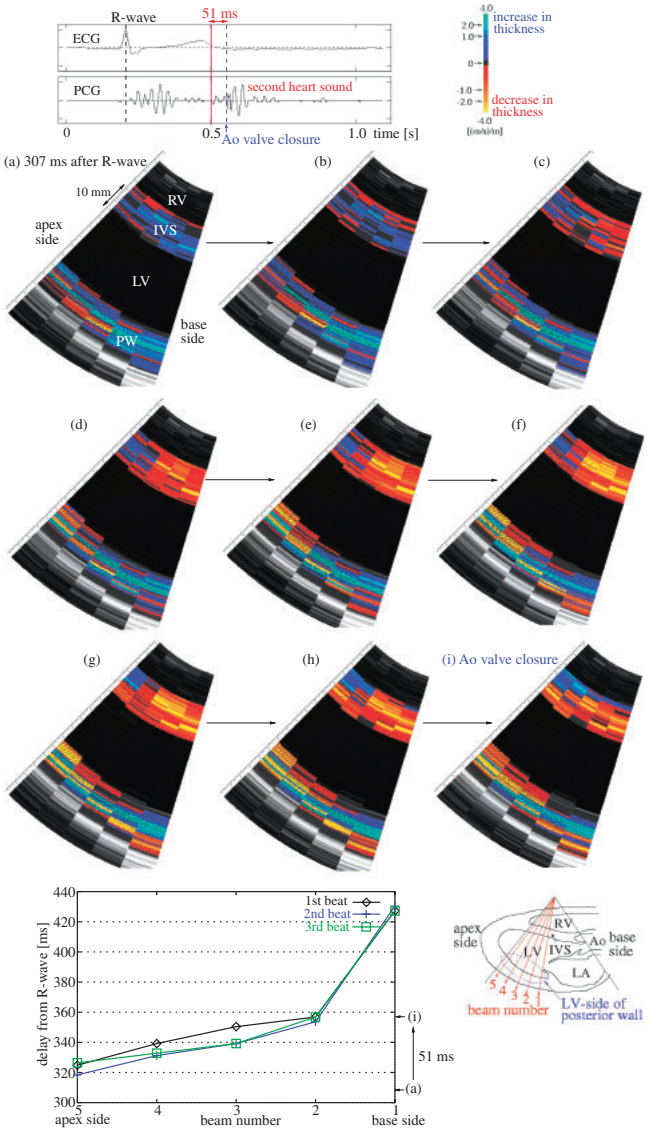

Fig. 4. Strain rate distribution during transitional period from contraction to relaxation every 6.3 ms around the second heart sound for the same subject as in Figs. 2 and 3. The lower graph shows the delay time from the R-wave to the time when the LV-side of the posterior wall along each ultrasonic beam is closest to the LV chamber.

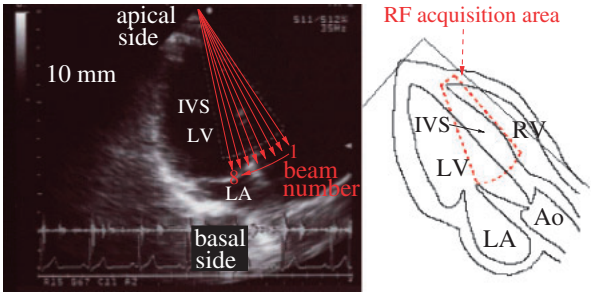

Fig. 5. Cross-sectional image of the left ventricle in the apical approach obtained by conventional echocardiography for a healthy 24-year-old male. The arrows show the directions of the eight ultrasonic beams used for estimating the strain rate distribution in the IVS.

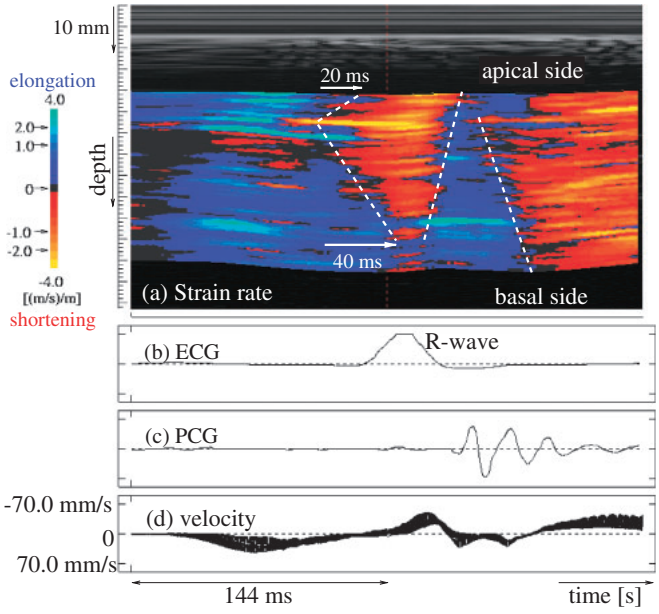

Fig. 6. Strain rate distribution in IVS along beam number 3 in Fig. 5 around R-wave. (a) Strain rate, $S_i(t)$, superimposed on M-mode image. (b) ECG. (c) PCG. (d) Superimposed estimates of velocity signals at multiple points along the beam.

dium in the transitional period from contraction to relaxation around the second heart sound every 6.3 ms in the long-axis view. It is recognized that the relaxation occurs from the basal area to the apical area in the IVS, and from the apical area to the basal area in the posterior wall. The transition from contraction to relaxation was found to precede the aortic (Ao) valve closure.[15] The bottom graph in Fig. 4 shows the delay time from the R-wave in the ECG to the time at which the endocardial side of the posterior wall along each ultrasonic beam shows the maximum inward displacement in the LV chamber. Each delay graph for three consecutive cardiac cycles is overlaid. The movement of the IVS and the posterior wall are away from and toward the probe on the chest during the cardiac systole, respectively, which shortens the LV chamber and causes blood to be pumped out.[11] Therefore, the translation of the IVS and the posterior wall is considered to be negligible. As shown in the graph, it was found that the apical area reaches the peak toward the LV chamber earlier than the basal area. This result corresponds to the transition in myocardial contraction/relaxation from the apical to the basal area in the posterior wall.

3.3 *Transition at beginning of contraction in IVS around R-wave in apical approach*

Figure 5 shows a cross-sectional image of the heart of a healthy 24-year-old male examined by the apical approach. For the acquisition of RF signals, 8 ultrasonic beams scanned the IVS, realizing a high frame rate of 560 Hz. The strain rate in the IVS was measured by the apical approach in order to investigate the transition at the beginning of contraction in the IVS.

The strain rate distribution along each ultrasonic beam was obtained by analyzing the region ± 144 ms ($= \pm 80$ frames) around the R-wave in the ECG. Figure 6 shows the strain rate distribution along beam number 3 in Fig. 5. Figure 6(a) shows strain rate $S_i(t)$, defined by eq. (2.1), superimposed on the M-mode image using the color code on the left-hand side of Fig. 6. Figures 6(b) and 6(c) show the ECG and PCG, respectively. Figure 6(d) shows superim-

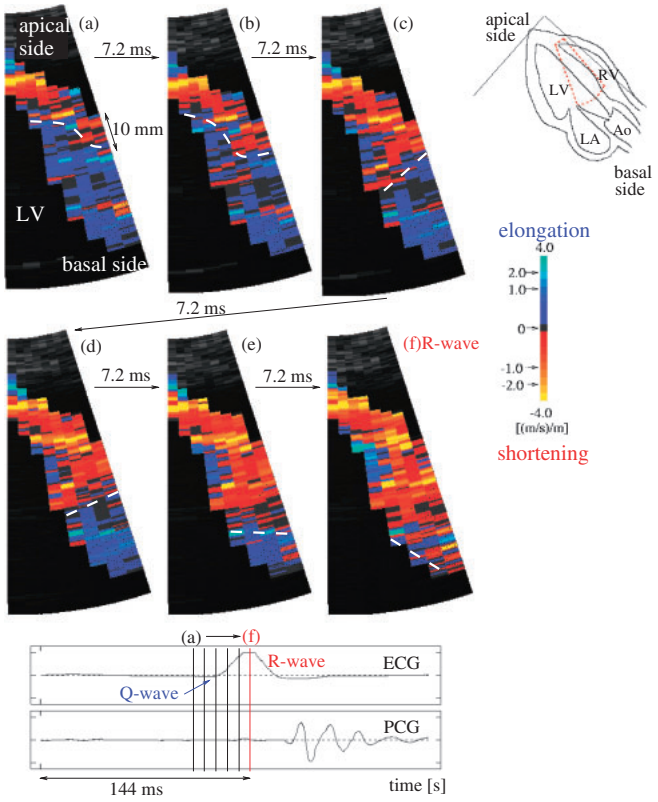

Fig. 7. Two-dimensional distribution of strain rate in IVS in apical approach every 7.2 ms around R-wave for the same subject as in Fig. 5. At (a) 36, (b) 29, (c) 22, (d) 14, and (e) 7 ms before the R-wave. (f) At the time of R-wave.

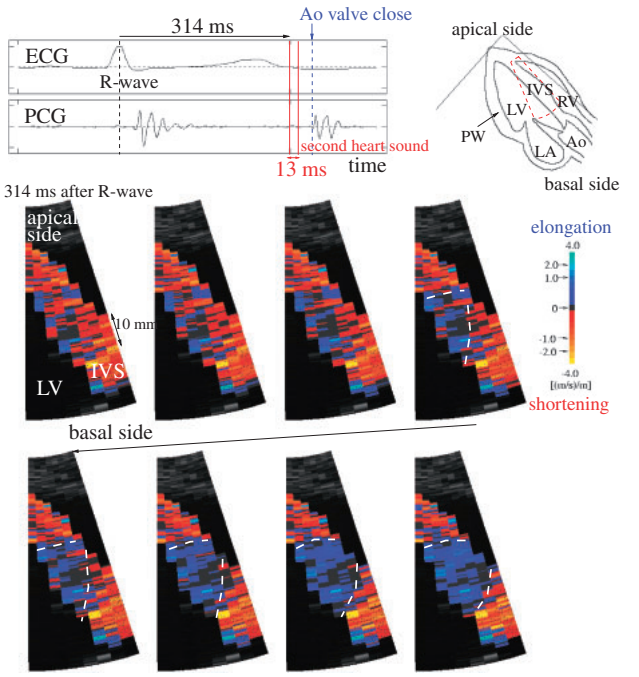

Fig. 8. Two-dimensional distribution of strain rate of IVS in apical approach every 1.8 ms around second heart sound for the same subject as in Fig. 5.

posed estimates of the velocity signals at multiple points in the IVS along the beam. In the apical approach, blue and red of the color code correspond to relaxation and contraction of the myocardium, respectively. In Fig. 6(a), it is seen that the contraction in the apical area precedes that in the basal area by about 40 ms just before the R-wave.

Figure 7 shows the spatial distribution of the strain rate of the IVS determined by the apical approach, around the R-wave for the same subject as shown in Figs. 5 and 6. It is recognized that myocardial contraction extends gradually from the apical area to the basal area just before the R-wave. The propagation speed of the contraction was found to be about 0.8 m/s. It is known that the propagation speed of electrically excited waves along the cardiac muscle is about 0.3–1 m/s.[16] Although the speed of the electrically excited wave and that of the observed propagation of cardiac rapid motion are in good agreement, the relationship between the electrically excited wave and the observed propagation is still unclear. The elucidation of this relationship requires further investigation, particularly the analysis of the posterior wall in the apical view. The electrical signal is conducted along the Purkinje fiber in the myocardium, which runs along the LV walls from the base side in the IVS to the base side in the posterior wall via the apical area.[16,17] Therefore, the simultaneous observation of both the IVS and the posterior wall in the apical view is needed to investigate the myocardial transition along the Purkinje fiber to obtain more information on this relationship. However, this mechanical contraction is found to occur around the Q-wave in the ECG, which is known to be the time of beginning of electrical excitation in the myocardium.[17] Therefore, this component is considered to be the first component of myocardial contraction in a cardiac cycle.

3.4 *Transition at beginning of relaxation in IVS around second heart sound in apical approach*

The spatial distribution of strain rate of the IVS around the second heart sound was obtained, as well as that around the R-wave. This period corresponds to the transient phase from myocardial contraction to relaxation. Figure 8 shows the transition from contraction to relaxation in the IVS around the second heart sound for the same subject as shown in Figs. 5–7. As seen in Fig. 8, myocardial relaxation occurs in the middle of the IVS in the late contraction phase, which extends gradually from the middle to both sides of the IVS.

3.5 *Comparison of results of apical approach with those in long-axis view*

The results obtained by the apical approach were compared with those in the long-axis view to confirm the transition of relaxation beginning from the middle of the IVS in the late ejection phase. Figure 9 shows the spatial distribution every 1.8 ms around the second heart sound for the same subject (Fig. 5) in the long-axis view. This period corresponds to that observed in Fig. 8. In the long-axis view, ultrasonic beams are almost perpendicular to those in the apical approach. Therefore, blue and red in the long-axis view correspond to contraction and relaxation, respectively.

Although the lateral resolution is low in the long-axis view in Fig. 9 because of the sparse scanning to achieve a high temporal resolution, the relaxation was found to extend from the middle to both sides of the IVS, as in the apical approach shown in Fig. 8.

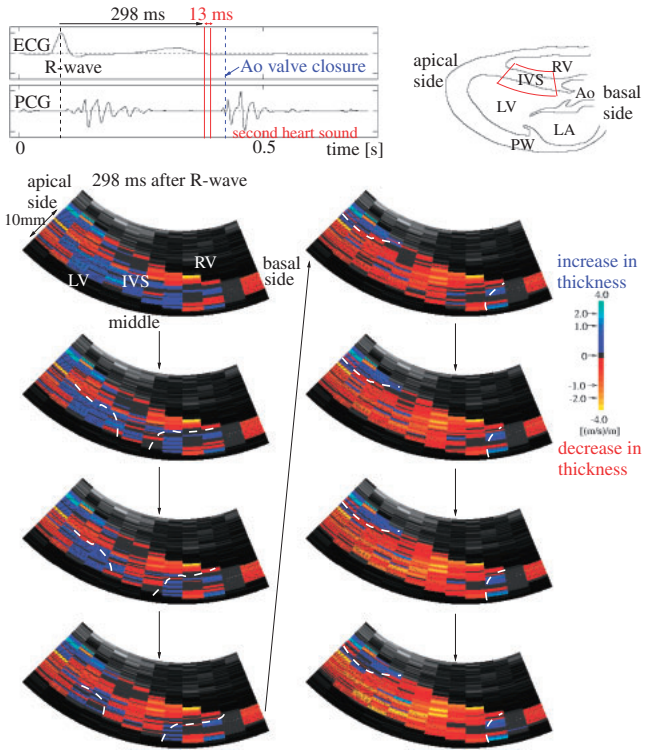

Fig. 9. Two-dimensional distribution of strain rate of IVS in long-axis view at every 1.8 ms around second heart sound for the same subject as in Fig. 5.

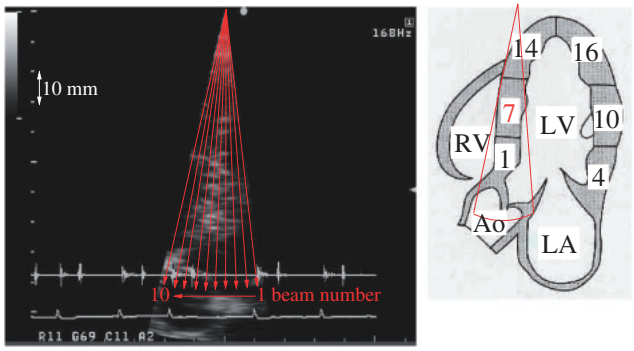

Fig. 10. Left: Cross-sectional image of left ventricle in apical approach obtained by conventional echocardiography for 79-year-old male with OMI. The arrows show the directions of the 10 ultrasonic beams used for the acquisition of RF signals in the IVS. Right: Segmentation in the apical long-axis view.[18)]

4. *In vivo* Experimental Results for Patient with Old Myocardial Infarction

As an example of noninvasive diagnosis of the myocardium, we applied the proposed method to examine the IVS of a 79-year-old male patient with old myocardial infarction (OMI). Figure 10 shows a cross-sectional image of the heart in the apical long-axis view obtained from the patient and the schematic of segmentation in the apical long-axis view.[18)] In the acquisition of RF signals, the ultrasonic beam scans 10 directions in the IVS and realizes a high frame rate of 490 Hz. During medical treatments, the infarcted region was found in the antero septal region (#7), as illustrated in Fig. 10.

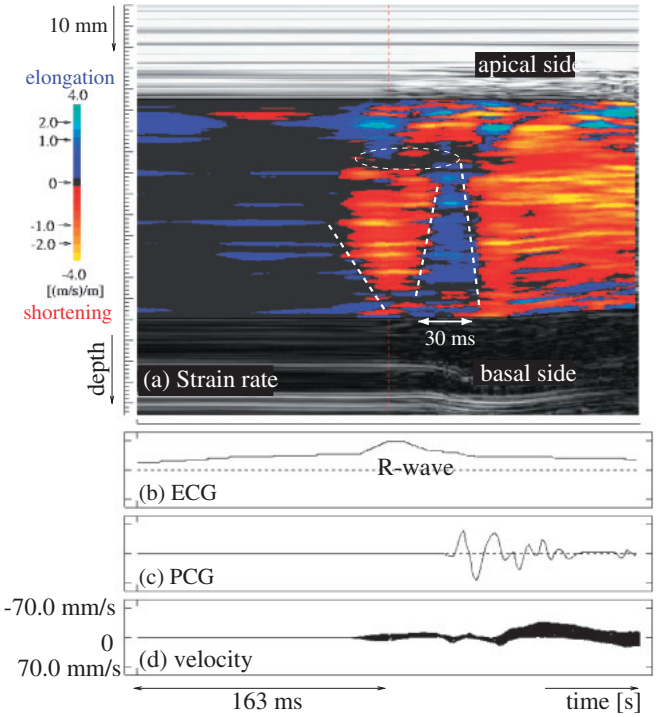

Fig. 11. Strain rate distribution in IVS along beam number 5 in Fig. 10 around R-wave. (a) Strain rate, $S_i(t)$, superimposed on M-mode image. (b) ECG. (c) PCG. (d) Superimposed estimates of velocity signals at multiple points along beam.

4.1 *Analysis around R-wave in ECG*

Beams 1-8 that scanned the IVS were analyzed. The strain rate distribution along each ultrasonic beam was obtained by analyzing the region ± 163 ms ($= \pm 80$ frames) around the R-wave in the ECG. Figure 11 shows the strain rate distribution along beam number 5 in Fig. 10. Results shown in Figs. 11(a)–11(d) correspond to those in Figs. 6(a)–6(d), respectively. From the strain rate distribution shown in Fig. 11(a), it was found that the elongation (blue) in the atrium contraction phase before the R-wave is smaller than that in the healthy subject shown in Fig. 6(a). Although transitional properties are similar to those for the healthy subject, the depth at which the strain rate is small was recognized around the R-wave [white dashed oval in Fig. 11(a)]. This region is further discussed in §4.3.

Figure 12 shows the spatial distribution of the strain rate of the IVS in the apical approach around the R-wave for the patient. These results correspond to those for the healthy subject shown in Fig. 7. It was found that myocardial contraction extends gradually from the apical area to the basal area just before the R-wave, as shown in Fig. 7. However, the region near the apical area in the IVS shows a small strain rate (grey zone), which is considered to result from a decrease in the ability to contract actively in the infarcted region.

4.2 *Analysis around second heart sound in PCG*

Figure 13 shows the transition from contraction to relaxation in the IVS around the second heart sound for the same patient as shown in Fig. 10. Figure 13 shows that the transitional properties in myocardial relaxation are similar to those of the healthy subject shown in Fig. 8. Relaxation occurs in the middle of the IVS in the late

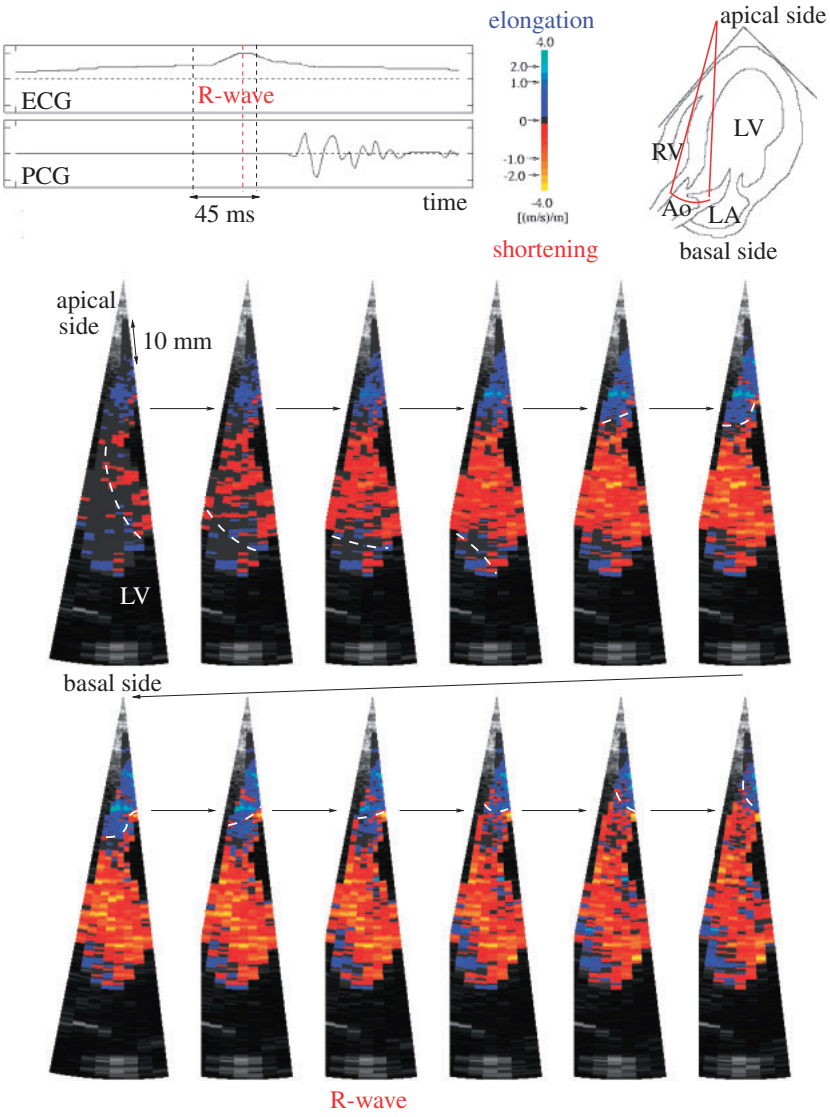

Fig. 12. Two-dimensional distribution of strain rate of IVS in apical approach every 4 ms around R-wave for same patient as in Fig. 10.

contraction phase, and extends gradually from the middle to both sides of the IVS.

The region near the apical area, which is gray in Fig. 12, shows a smaller strain rate relative to that in the surrounding area, but no definite difference was recognized around the second heart sound.

4.3 Average magnitudes of strain rates around R-wave and second heart sound

To evaluate how each region in the IVS contracts/relaxes in the transitional period, we adopted the average magnitude of strain rate. Figure 14 shows color-coded images of average strain rate in the periods around the R-wave in the ECG and second heart sound in the PCG. Figure 14(a) shows the average magnitude of strain rate for the period ± 82 ms (± 40 frames) around the R-wave. As shown in Fig. 14(c), the period around the second heart sound was analyzed as well as that around the R-wave. These periods correspond to the transitional period in myocardial contraction and relaxation. Figures 14(b) and 14(d) show the B-mode image at the R-wave and that at the Ao valve closure, respectively. In each period, two consecutive cardiac cycles were analyzed.

In Fig. 14(a), it was found that the region surrounded by the white dashed line near the apical area in Fig. 14(b) shows a small average strain rate. This region corresponds to the region where the propagation of contraction was not observed in Fig. 12. This indicates that the thickness of the region changes negligibly around the R-wave, which is considered to result from the decrease in the ability to contract actively in the infarcted region.

As for the period around the second heart sound [Fig. 14(c)], the infarcted region was not clearly distinguished from the surrounding area. The infarcted area is considered to be passively stretched due to the filling of the left ventricle with blood. Therefore, in the evaluation of the myocardial function using the strain rate, it is useful to evaluate the strain rate in the period around the R-wave. In this period, the mechanical reaction of the myocardium due to electrical excitement can be sensitively evaluated from the strain rate.

4.4 Comparison of healthy subject with patient

As discussed in §4.3, the infarcted area was clearly distinguished from the normal area in the period around the

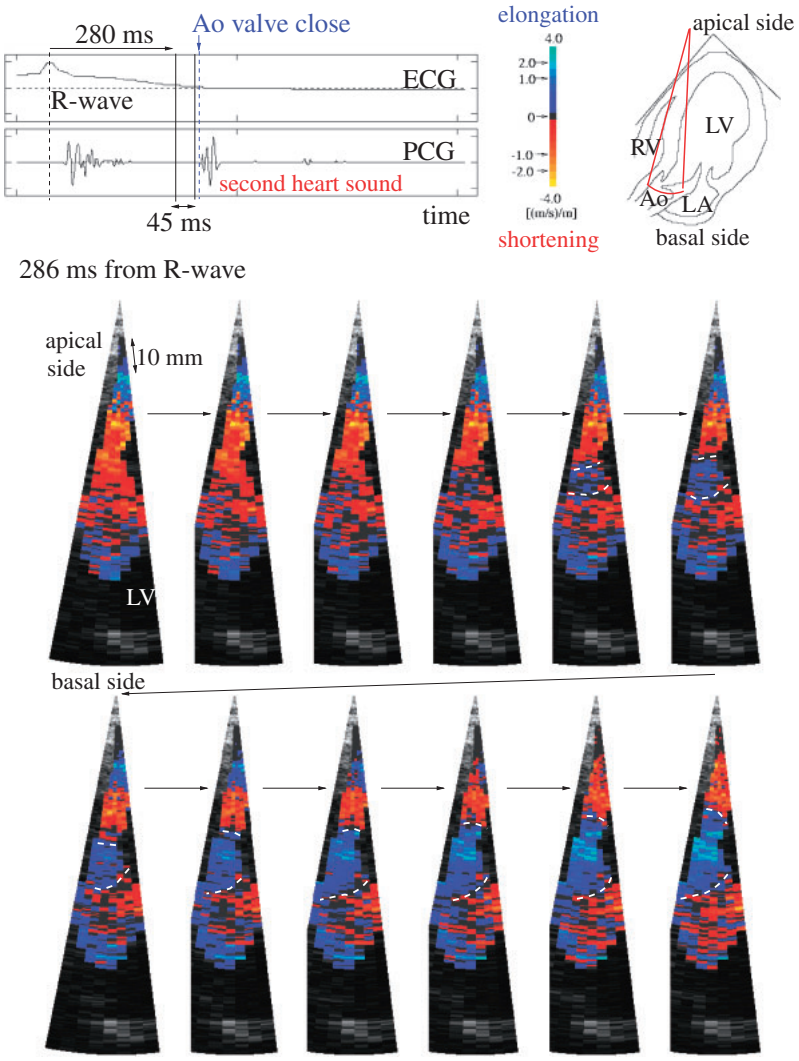

Fig. 13. Two-dimensional distribution of strain rate of IVS in apical approach every 4 ms around second heart sound for same patient as in Fig. 10.

R-wave. Here, the results of the patient are compared with those of the healthy subject in the period around the R-wave. Figure 15 shows the color-coded image of the average magnitude of strain rate for the period ±82 ms around the R-wave. Figures 15(a) and 15(b) are the results for the healthy subject shown in Fig. 5 and the patient with OMI shown in Fig. 10, respectively. In Figs. 15(a) and 15(b), the cross-sectional images were mirror images in the horizontal direction, but almost the same areas in the IVS were analyzed.

Upon comparing Fig. 15(a) with Fig. 15(b), strain in the patient is found to be smaller than that in the healthy subject on the whole. In addition, a local region with a small change in thickness was observed in the patient but not in the healthy subject. These results indicate the possibility of using this method to quantitatively detect a locally infarcted region in the myocardium.

5. Conclusions

The spatial distribution of myocardial strain rate was measured at an extremely high temporal resolution of a frame rate of about 600 Hz. From *in vivo* experimental results in the long-axis view, it was found that the spatial properties of myocardial contraction and relaxation vary continuously. In particular, the transitional properties in myocardial contraction/relaxation from the apical area to the basal area were observed in the posterior wall. These continuous transitions probably contribute to efficient functioning of the human heart. In addition, the left ventricle was measured not only in the long-axis view but also by the apical approach. The spatial distribution of the strain rate of the IVS in the apical approach showed transitions of myocardial contraction and relaxation in the IVS and the posterior wall. These results indicate the possibility of using this method for the elucidation of the mechanism of myocardial contraction and relaxation.

In addition, this method was applied to a patient with OMI. It was found that the infarcted area could clearly be distinguished from a normal area in the period around the R-wave in the ECG. This result indicates the possibility of using this method for noninvasive diagnosis of the myocardium, particularly the detection of a locally infarcted region in the myocardium, which is difficult to detect using the ECG.[19)]

Acknowledgements

The authors are grateful to associate professor Yoshifumi Saijo of Institute of Development, Aging and Cancer,

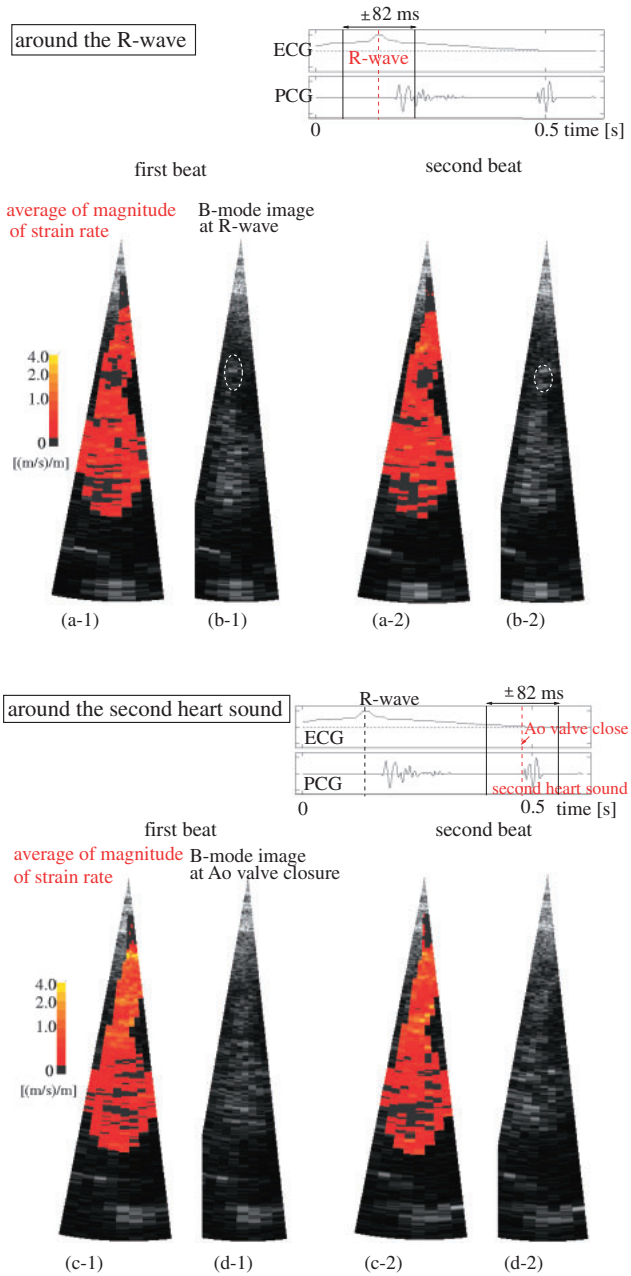

Fig. 14. Two-dimensional distribution of average magnitude of strain rate around R-wave and second heart sound. (1) First heart beat. (2) Second heart beat. (a) Average magnitude of strain rate for the period ±82 ms around R-wave. (b) B-mode image at R-wave. (c) Average magnitude of strain rate for the period ±82 ms around Ao valve closure (second heart sound). (d) B-mode image at Ao valve closure.

Tohoku University, and Dr. Sachiko Watanabe of Tohoku University Hospital for helpful discussion and assistance with experiments.

1) G. R. Sutherland, G. D. Salvo, P. Claus, J. D'hooge, and B. Bijnens: J. Am. Soc. Echocardiogr. **17** (2004) 788.
2) G. R. Sutherland, M. J. Stewart, K. W. Groundstroem, C. M. Moran, A. Fleming, F. J. Guell-Peris, R. A. Riemersma, L. N. Fenn, K. A. Fox, and W. N. McDicken: J. Am. Soc. Echocardiogr. **7** (1994) 441.
3) A. Heimdal, A. Støylen, H. Torp, and T. Skjarpe: J. Am. Soc. Echocardiogr. **11** (1998) 1013.
4) K. Miyatake, M. Yamagushi, N. Tanaka, M. Uematsu, N. Yamazaki, Y. Mine, A. Sano, and M. Hirama: J. Am. College Cardiol. **25** (1995) 717.
5) P. Palka, A. Lange, A. D. Fleming, G. R. Sutherland, L. N. Fenn, and W. N. McDicken: J. Am. Soc. Echocardiogr. **8** (1995) 659.
6) J. Gorcsan III, V. K. Gulati, W. A. Mandarino, and W. E. Katz: Am. Heart J. **131** (1996) 1203.
7) H. Yoshiara, H. Hasegawa, H. Kanai, and M. Tanaka: Proc. Spring Meet. Acoustical Society of Japan, 2006, p. 1131 [in Japanese].
8) H. Yoshiara, H. Hasegawa, H. Kanai, and M. Tanaka: to be published in Cho-onpa Igaku **34** (2007) [in Japanese].
9) H. Kanai, M. Sato, Y. Koiwa, and N. Chubachi: IEEE Trans. Ultrason. Ferroelectr. Freq. Control **43** (1996) 791.
10) H. Kanai, H. Hasegawa, N. Chubachi, Y. Koiwa, and M. Tanaka: IEEE Trans. Ultrason. Ferroelectr. Freq. Control **44** (1997) 752.
11) H. Kanai, Y. Koiwa, Y. Saito, I. Susukida, and M. Tanaka: Jpn. J. Appl. Phys. **38** (1999) 3403.
12) H. Kanai, Y. Koiwa, S. Katsumata, N. Izumi, and M. Tanaka: Jpn. J. Appl. Phys. **42** (2003) 3239.
13) H. Kanai, H. Hasegawa, and K. Imamura: Jpn. J. Appl. Phys. **45** (2006) 4718.
14) J. D'hooge, E. Konofagou, F. Jamal, A. Heimidal, L. Barrios, B. Bijnens, J. Thoen, F. V. Werf, G. R. Sutherland, and P. Suetens: IEEE Trans. Ultrason. Ferroelectr. Freq. Control **49** (2002) 281.
15) H. Kanai, S. Yonechi, I. Susukida, Y. Koiwa, H. Kamada, and M. Tanaka: Ultrasonics **38** (2000) 405.
16) D. M. Bers: *Excitation–Contraction Coupling and Cardiac Contractile Force* (Kluwer Academic, Boston, 2001) p. 64.
17) F. Netter: *The CIBA Collection of Medical Illustrations Heart* (Ciba Geigy Japan, Takarazuka, 1975) p. 49.
18) N. B. Schiller, P. M. Shah, M. Crawford, A. De Maria, R. Devereux, H. Feigenbaum, H. Gutgesell, N. Reicheck, D. Sahn, I. Schnittger, N. H. Silverman, and A. J. Tajik: J. Am. Soc. Echocardiogr. **2** (1989) 358.
19) F. Netter: *The CIBA Collection of Medical Illustrations Heart* (Ciba Geigy Japan, Takarazuka, 1975) p. 62.

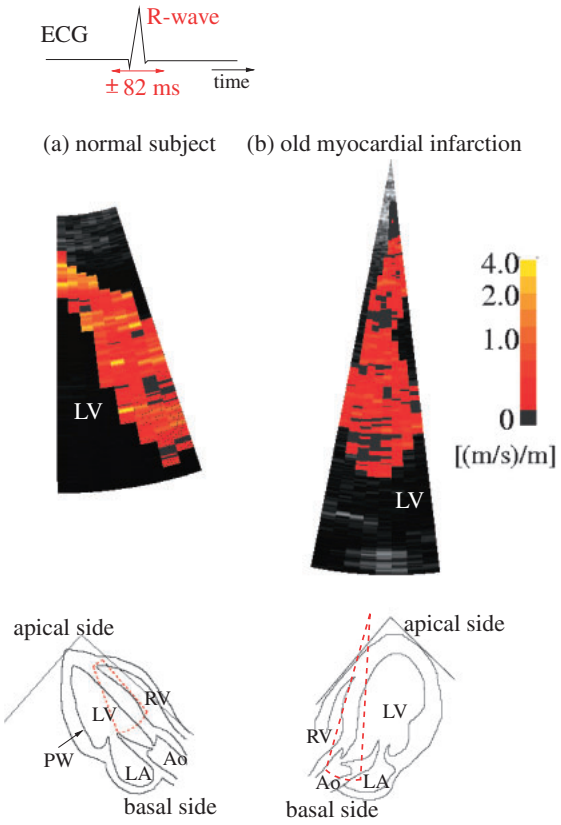

Fig. 15. Average magnitudes of strain rates of the healthy subject and the patient in the period ±82 ms around R-wave in ECG. (a) Healthy subject as in Fig. 5. (b) Same patient with old myocardial infarction as in Fig. 10.